frontiers in Oncology

ORIGINAL RESEARCH
published: 29 April 2021
doi: 10.3389/fonc.2021.621993

Ultrasound-Based Radiomics Analysis for Predicting Disease-Free Survival of Invasive Breast Cancer

Lang Xiong[1†], Haolin Chen[2,3,4†], Xiaofeng Tang[5†], Biyun Chen[1], Xinhua Jiang[1], Lizhi Liu[1], Yanqiu Feng[2,3,4], Longzhong Liu[5] and Li Li[1*]*

[1] Department of Medical Imaging, Collaborative Innovation Center for Cancer Medicine, State Key Laboratory of Oncology in South China, Sun Yat-Sen University Cancer Center, Guangzhou, China, [2] School of Biomedical Engineering, Southern Medical University, Guangzhou, China, [3] Guangdong Provincial Key Laboratory of Medical Image Processing, Southern Medical University, Guangzhou, China, [4] Guangdong-Hong Kong-Macao Greater Bay Area Center for Brain Science and Brain-Inspired Intelligence, Southern Medical University, Guangzhou, China, [5] Department of Ultrasound, Collaborative Innovation Center for Cancer Medicine, State Key Laboratory of Oncology in South China, Sun Yat-Sen University Cancer Center, Guangzhou, China

Background: Accurate prediction of recurrence is crucial for personalized treatment in breast cancer, and whether the radiomics features of ultrasound (US) could be used to predict recurrence of breast cancer is still uncertain. Here, we developed a radiomics signature based on preoperative US to predict disease-free survival (DFS) in patients with invasive breast cancer and assess its additional value to the clinicopathological predictors for individualized DFS prediction.

Methods: We identified 620 patients with invasive breast cancer and randomly divided them into the training (n = 372) and validation (n = 248) cohorts. A radiomics signature was constructed using least absolute shrinkage and selection operator (LASSO) Cox regression in the training cohort and validated in the validation cohort. Univariate and multivariate Cox proportional hazards model and Kaplan–Meier survival analysis were used to determine the association of the radiomics signature and clinicopathological variables with DFS. To evaluate the additional value of the radiomics signature for DFS prediction, a radiomics nomogram combining the radiomics signature and clinicopathological predictors was constructed and assessed in terms of discrimination, calibration, reclassification, and clinical usefulness.

Results: The radiomics signature was significantly associated with DFS, independent of the clinicopathological predictors. The radiomics nomogram performed better than the clinicopathological nomogram (C-index, 0.796 *vs.* 0.761) and provided better calibration and positive net reclassification improvement (0.147, P = 0.035) in the validation cohort. Decision curve analysis also demonstrated that the radiomics nomogram was clinically useful.

OPEN ACCESS

Edited by:
Shengtao Zhou,
Sichuan University, China

Reviewed by:
Isabella Castellano,
University of Turin, Italy
Fa Zhang,
Institute of Computing Technology, Chinese Academy of Sciences (CAS), China

***Correspondence:**
Longzhong Liu
liulzh@sysucc.org.cn
Li Li
li2@mail.sysu.edu.cn

[†]These authors have contributed equally to this work

Specialty section:
This article was submitted to Women's Cancer, a section of the journal Frontiers in Oncology

Received: *27 October 2020*
Accepted: *06 April 2021*
Published: *29 April 2021*

Citation:
Xiong L, Chen H, Tang X, Chen B, Jiang X, Liu L, Feng Y, Liu L and Li L (2021) Ultrasound-Based Radiomics Analysis for Predicting Disease-Free Survival of Invasive Breast Cancer. Front. Oncol. 11:621993. doi: 10.3389/fonc.2021.621993

Conclusion: US radiomics signature is a potential imaging biomarker for risk stratification of DFS in invasive breast cancer, and US-based radiomics nomogram improved accuracy of DFS prediction.

Keywords: breast cancer, radiomics, ultrasound, disease-free survival, nomogram

INTRODUCTION

Recurrence remains the principal cause of breast cancer-related death, which seriously endanger the health of women (1, 2). More intensive therapy seems to improve prognosis for patients at high risk of recurrence (3). For predicting breast cancer recurrence, many prognostic models have been developed based on the clinicopathological factors like tumor size, nodal status, and Ki-67 expression, but the performance of most models declined for some independent populations (4). Gene tests have been reported to predict patient outcome (5), but they are difficult to be widely used in clinically due to the high price and complex operation. More convenient and appropriate methods to enhance recurrence prediction for breast cancer is the need of the hour.

Radiomics holds promise in predicting breast cancer recurrence due to its high-dimensional features extracted from medical images (6), which are not only related to the multigene assay recurrence scores of breast cancer but also associated to the recurrence survival (7–9). However, most previous studies about radiomics and breast cancer survival conducted thus far were based on magnetic resonance imaging (MRI). Ultrasound (US) is a safe, inexpensive, and widely available modality. US radiomics features could distinguish benign breast tumors from malignant tumors, could predict axillary lymph node metastasis, and could assist clinicians with accurate prognosis prediction in breast cancer (10–12). Therefore, whether US radiomics features could be used to predict breast cancer recurrence is merits further investigation.

Considering the above findings, a multiple-feature-based radiomics signature extracted from preoperative US images was developed for predicting disease-free survival (DFS) of invasive breast cancer in our study and its additional value added to the clinicopathological predictor was further assessed.

MATERIALS AND METHODS

Patients

This study has obtained the ethical approval from the institutional review board, the informed patient consent was waived due to the nature of retrospective analysis. From February 2014 to November 2016, 812 consecutive women of breast cancer were identified. The inclusion criteria included: (1) patients with complete clinicopathological data and follow-up information; (2) primary unilateral invasive breast cancer confirmed by histopathology; (3) US examination performed within 2 weeks preoperatively (4); patients with no anticancer therapy before US examination; and (5) patients without history of breast cancer and/or other malignancy. The exclusion criteria included: (1) patients who received preoperative neoadjuvant chemotherapy; (2) patients presenting with metastatic disease; (3) insufficient quality of images and/or only partial tumor included in the images; and (4) patients lost to follow up. Finally, we enrolled 620 patients (mean age: 49.62 years, range: 27–87 years) (**Figure S1**) and divided them into the training cohort (n = 372) and validation cohort (n=248) randomly.

Clinicopathological Data

Medical records were reviewed to acquire the clinical and pathological data, including: age; status of menopausal; history of risk factors for breast cancer (including family history of breast cancer and/or benign breast disease history); surgery type and adjuvant treatment (radiotherapy, chemotherapy, endocrine therapy, targeted therapy); pathologic tumor size; histologic type; TNM stage; T stage; N stage; lymphovascular invasion (LVI); invasion of nerves; associated ductal carcinoma *in situ* (DCIS); and status of estrogen receptor (ER), progesterone receptor (PR), human epidermal growth factor receptor 2 (HER2), and Ki-67, which were assessed by immunohistochemistry (IHC) and fluorescence *in situ hybridization* (FISH). ER/PR was defined as positive if nuclear staining was present in ≥1% cells (13). The HER2 status was scored as 0, 1+, 2+, or 3+. Scores 0 and 1+ were defined as negative, and score 3+ as positive. Score 2+ was considered indeterminate and was further confirmed with FISH (14). According to results of IHC and FISH, tumors were categorized into the following four subtypes: luminal A, luminal B, HER2-enriched and triple-negative (15). The targeted therapy was anti-HER2 therapy using trastuzumab. The American Joint Committee on Cancer TNM Staging Manual, 7th edition (16), was used for tumor stage.

Follow-Up

DFS was considered as the end point of the present study, which was defined as the interval time between the surgery and recurrence or breast cancer-related death, whichever came first. Recurrence means locoregional recurrence, distant metastasis, or contralateral breast cancer (17). Physical examination, histopathology, and imaging modalities such as US, computed tomography, MRI were used to demonstrated the recurrence. At the last follow-up, patients without an event and/or died of non-breast cancer related events were censored; two patients died from cardiovascular disease in this study.

Imaging Acquisition, Radiomics Analysis and Radiomics Signature Construction

Figure S2 shows the radiomics workflow. US images were collected in different machines (**Table S1**) and exported from

the data system of our hospital. Radiologist 1 (6 years' experience) selected one greyscale image with the largest cross-section for every breast tumor, and drew a single region-of-interest (ROI) along the tumor margin by Photoshop software (**Figure S3**). Then, the ROIs were validated by radiologist 2 (10 years' experience). The radiologists did not know the results of pathology. For multifocal (MF) or multicentric (MC) disease (18), we chose the largest tumor to analysis. After the ROIs were defined, radiomics features which could be divided into four categories, including first-order statistics features, two-dimensional (2D) shape-based features, texture features, and wavelet features, were extracted using the "PyRadiomics" package in Python software (19). Then, a two-step feature selection method which comprised by Sperman correlation coefficients and Ward linkage method, and least absolute shrinkage and selection operator (LASSO) Cox method were performed (20, 21). Finally, a radiomics signature was constructed, and a radiomics score (Rad-score) was calculated at the same time. In the supplementary materials, there are more details.

The intra-observer agreement of feature extraction was evaluated by inter-class correlation coefficient (ICC). We randomly selected 95 patients and redrew ROIs by radiologist 1 one month later after the first ROI segmentation. An ICC >0.75 indicated a good reproducibility.

Validation of Radiomics Signature

In order to assess the association of the radiomics signature with DFS, patients were divided into a high risk and a low risk groups using the cutoff of the Rad-score identified by X-tile (22). We performed Kaplan–Meier survival analysis to analyze DFS between these two groups and the differences of survival curves were determined by Log-rank tests. We also assessed the association of the single selected feature with DFS by the same way. Then, distribution of Rad-score and DFS along with the selected features' expression were assessed. Stratified analyses were performed using subgroups within the molecular subtype and categorical clinicopathological variables.

The univariate Cox proportional hazards model was used to analyze the effects of the clinicopathological variables and radiomics signature on DFS. Then, the most useful predictors were selected using multivariate Cox proportional hazards model by including clinicopathological variables in a step-wise (forward and backward) manner based on the Bayesian information criterion (BIC). Finally, the radiomics signature was integrated into a multivariable Cox proportional hazards model to evaluate its performance in DFS prediction.

All the above analyses were first performed in the training cohort, and then validated in the validation cohort, except for the stratified analyses which were performed in the whole cohort.

The Additional Value of Radiomics Signature for DFS Prediction

In order to evaluate the additional value of the radiomics signature for DFS prediction, a radiomics nomogram containing the radiomics signature and clinicopathological predictors was constructed and compared with a clinicopathological nomogram containing only the clinicopathological predictors. The performance of the nomogram was assessed in the following four aspects: (1) discrimination, it was evaluated by Harrell's concordance index (C-index) (23); (2) calibration curves, they were generated to compare the predicted *vs.* actual survival; (3) reclassification, the improvement of usefulness added by the radiomics signature was quantified by net reclassification improvement (NRI) (24); (4) clinical usefulness, it was determined by decision curve analysis (DCA) (25). In addition, the goodness-of-fit of all the models were assessed by the likelihood ratio test and BIC.

Subgroup Analyses Based on Ultrasound Machines

To investigate whether different sonographic platforms affect the performance of radiomics signature for DFS prediction, we repeated Kaplan–Meier survival analysis in patients examined at GE healthcare and Mindray US systems, which were the most frequently used machines in this study.

Statistical Analysis

Python software (Python Language Reference, version 3.6.9. Available at http://www.python.org) and R statistical software (version 4.0.0; R Foundation for Statistical Computing, Vienna, Austria) were used for all the statistical analyses. Chi-squared or Fisher's exact test and Mann–Whitney U test were used to assess differences in distributions for categorical variables and continuous variables, respectively. The "lifelines" package was used for Kaplan–Meier survival analysis, log-rank test, and Cox regression. The "rms" package was used for the nomogram construction and calibration. NRI was calculated by "survIDINRI" package. The "rmda" package was used for DCA. A bilateral P value < 0.05 was considered significant.

RESULTS

DFS and Clinicopathological Characteristics

The median period of follow-up was 48.99 (interquartile range [IQR], 44.42–62.98) months. Events occurred in 80 patients (80/620, 12.90%), including: 40 distant metastases; 17 locoregional recurrences; 12 locoregional recurrences and distant metastases; seven contralateral breast cancer (six invasive breast cancer and one DCIS); and four breast cancer-related death. The median DFS was 22.29 (IQR, 14.52–33.84) months. The comparison of the clinicopathological characteristics in the training and validation cohorts showed no significantly differences (**Table 1**).

The Radiomics Signature Construction and Validation

The mean ICC based on twice feature extraction was 0.824 (range, 0.798–0.999), which means the high intra-observer agreement for the radiomics feature extraction. Thence, all findings were based on the first feature extraction.

TABLE 1 | Characteristics of patients in the training and validation cohorts.

Characteristics	Training cohort (n = 372)	Validation cohort (n = 248)	*P*-value
Age, (years)[a]	49.10 ± 10.46	50.41 ± 10.76	0.094
Menopausal status	238 (63.98)	159 (64.11)	0.973
Premenopausal	134 (36.02)	89 (35.89)	
Menopause			
History of risk factors for breast cancer[b]	359 (96.51)	240 (96.77)	0.856
No	13 (3.49)	8 (3.23)	
Yes			
Pathologic tumor size (cm)[a]	2.62 ± 1.40	2.51 ± 1.24	0.416
Molecular subtype	76 (20.43)	46 (18.55)	0.571
Luminal A	204 (54.84)	130 (52.42)	
Luminal B	55 (14.78)	39 (15.73)	
HER2-enriched	37 (9.95)	33 (13.31)	
Triple-negative			
TNM stage	90 (24.19)	78 (31.45)	0.132
I	196 (52.69)	116 (46.77)	
II	86 (23.12)	54 (21.77)	
III			
T stage	159 (42.74)	116 (46.77)	0.434[d]
1	193 (51.88)	123 (49.60)	
2	15 (4.03)	8 (3.23)	
3	5 (1.34)	1 (0.40)	
4			
N stage	178 (47.85)	126 (50.81)	0.847
0	113 (30.38)	73 (29.44)	
1	53 (14.25)	34 (13.71)	
2	28 (7.53)	15 (6.05)	
3			
ER status	96 (25.81)	74 (29.84)	0.270
Negative	276 (74.19)	174 (70.16)	
Positive			
PR status	113 (30.38)	94 (37.90)	0.052
Negative	259 (69.62)	154 (62.10)	
Positive			
HER2 status	255 (68.55)	163 (65.73)	0.463
Negative	117 (31.45)	85 (34.27)	
Positive			
Ki-67 status	292 (78.49)	196 (79.03)	0.873
>14%	80 (21.51)	52 (20.97)	
≤14%			
Lymphovascular invasion	239 (64.25)	159 (64.11)	0.973
Absent	133 (35.75)	89 (35.89)	
Present			
Invasion of nerves	305 (81.99)	206 (83.06)	0.730
Absent	67 (18.01)	42 (16.94)	
Present			
Associated ductal carcinoma in situ	274 (73.66)	180 (72.58)	0.767
Absent	98 (26.34)	68 (27.42)	
Present			
Multifocal/multicentric disease	361 (97.04)	240 (96.77)	0.849
No	11 (2.96)	8 (3.23)	
Yes			
Histology type	346 (93.01)	227 (91.53)	0.772
invasive ductal carcinoma	12 (3.23)	9 (3.63)	
invasive lobular carcinoma	14 (3.76)	12 (4.84)	
Others[c]			
Type of surgery	322 (86.56)	222 (89.52)	0.271
Mastectomy	50 (13.44)	26 (10.48)	
breast conservation surgery			
Adjuvant endocrine therapy	113 (30.38)	85 (34.27)	0.308
No	259 (69.62)	163 (65.73)	
Yes			
Adjuvant chemotherapy	75 (20.16)	53 (21.37)	0.715
No	297 (79.84)	195 (78.63)	
Yes			
Adjuvant radiation	239 (64.25)	156 (62.90)	0.733
No	133 (35.75)	92 (37.10)	
Yes			
Adjuvant targeted therapy	315 (84.68)	208 (83.87)	0.787
No	57 (15.32)	40 (16.13)	
Yes			

Unless stated otherwise, data are numbers of patients, with percentages in parentheses.
[a]Data represent mean ± standard deviations.
[b]History of risk factors for breast cancer include six patients with family history of breast cancer, 14 patients with benign breast disease history, one patient with breast lesion biopsy history.
[c]Other cancers include 13 mucinous carcinomas, five papillary carcinomas, three medullary carcinomas, two metaplastic carcinomas, one tubular carcinoma, one cribriform carcinoma, one apocrine carcinoma.
[d]P value is calculated after combining T3 and T4 as one group because more than 20% of the expected frequencies are less than 5.

Totally, 14 features were selected from 1209 features to build radiomics signature in the training cohort (**Table S2** and **Figure S4**) and only one of them could distinguish patients with different prognoses (**Figures S5**, **S6**). The radiomics signature showed moderate performance on DFS estimation both in the training (C-index, 0.714; 95% confidence interval [CI], 0.63–0.80) and validation (C-index, 0.632; 95% CI, 0.52–0.74) cohorts. Based on the cutoff (1.816) of Rad-score (**Figure S7**), patients with higher Rad-score (≥1.816) were divided into the high-risk group, whereas patients with lower Rad-score (<1.816) were divided into the low-risk group, and their characteristics are shown in **Table 2**.

The Rad-score prognostic accuracy determined by time-dependent receiver operator characteristics (ROC) curves and Kaplan–Meier survival curves are shown in **Figure 1**. The radiomics signature was significantly associated with DFS in the training ($P < 0.0001$) and validation ($P = 0.003$) cohorts. The 5-year DFS of the high- and low-risk groups were 61.27% and 90.10% in the training cohort and 76.60 and 87.07% in the validation cohort, respectively. The distribution of the Rad-score and DFS are shown in **Figures S8**–**S9**, patients with higher Rad-score were more likely to experience events.

Results of stratified analysis based on molecular subtype are shown in **Figure 2**. The Rad-score successfully discriminate prognoses in luminal B ($P = 0.00006$) and triple-negative ($P = 0.00003$), but failed in either luminal A ($P = 0.563$) or HER2-enriched ($P = 0.109$). The radiomics signature remained a statistically and clinically predictor in most subgroups based on clinicopathological variables (**Figure S10**).

TABLE 2 | Characteristics of patients according to the risk group based on radiomics signature in the training and validation cohorts.

Characteristics	Training cohort (n = 372)			Validation cohort (n = 248)		
	High-risk (n = 54)	Low-risk (n = 318)	*P*-value	High-risk (n = 50)	Low-risk (n = 198)	*P*-value
Rad-score	2.09 ± 0.21	1.37 ± 0.28	<0.0001	2.12 ± 0.30	1.30 ± 0.41	<0.0001
Age, (years)[a]	50.83 ± 11.15	48.80 ± 10.31	0.220	51.34 ± 10.72	50.17 ± 10.76	0.513
Menopausal status	29 (53.70)	222 (69.81)	0.019	29 (58)	117 (59.09)	0.889
Premenopausal	25 (46.30)	96 (30.19)		21 (42)	81 (40.91)	
Menopause						
History of risk factors for breast cancer[b]	51 (94.44)	308 (96.86)	0.623	47 (94)	193 (97.47)	0.427
No	3 (5.56)	10 (3.14)		3 (6)	5 (2.53)	
Yes						
Pathologic tumor size (cm)[a]	3.46 ± 1.48	2.48 ± 1.33	<0.0001	3.14 ± 1.36	2.35 ± 1.15	0.00001
Molecular subtype	6 (11.11)	72 (22.64)	0.043	5 (10)	39 (19.70)	0.042
Luminal A	39 (72.22)	169 (53.14)		23 (46)	103 (52.02)	
Luminal B	7 (12.96)	44 (13.84)		15 (30)	28 (14.14)	
HER2-enriched	2 (3.70)	33 (10.38)		7 (14)	28 (14.14)	
Triple-negative						
TNM stage	6 (11.11)	84 (26.42)	0.024	7 (14)	71 (35.86)	0.0004
I	30 (55.56)	166 (52.20)		23 (46)	93 (46.97)	
II	18 (33.33)	68 (21.38)		20 (40)	34 (17.17)	
III						
T stage	9 (16.67)	150 (47.17)	<0.0001[d]	9 (18)	107 (54.04)	<0.0001[d]
1	37 (68.52)	156 (49.06)		36 (72)	87 (43.94)	
2	5 (9.26)	10 (3.14)		4 (8)	4 (2.02)	
3	3 (5.56)	2 (0.63)		1 (2)	0 (0.00)	
4						
N stage	17 (31.48)	161 (50.62)	0.016	21 (42)	105 (53.03)	0.039
0	22 (40.74)	91 (28.62)		12 (24)	61 (30.81)	
1	7 (12.96)	46 (14.47)		11 (22)	23 (11.62)	
2	8 (14.81)	20 (6.29)		6 (12)	9 (4.55)	
3						
ER status	17 (31.48)	79 (24.84)	0.303	16 (32)	58 (29.29)	0.709
Negative	37 (68.52)	239 (75.16)		34 (68)	140 (70.71)	
Positive						
PR status	19 (35.19)	94 (29.56)	0.406	21 (42)	73 (36.87)	0.504
Negative	35 (64.81)	224 (70.44)		29 (58)	125 (63.13)	
Positive						
HER2 status	32 (59.26)	223 (70.13)	0.112	32 (64)	131 (66.16)	0.774
Negative	22 (40.74)	95 (29.87)		18 (36)	67 (33.84)	
Positive						
Ki-67 status	49 (90.74)	243 (76.42)	0.018	42 (84)	154 (77.78)	0.334
>14%	5 (9.26)	75 (23.58)		8 (16)	44 (22.22)	
≤14%						
Lymphovascular invasion	25 (46.30)	214 (67.30)	0.003	23 (46)	136 (68.69)	0.003
Absent	29 (53.70)	104 (32.70)		27 (54)	62 (31.31)	
Present						
Invasion of nerves	43 (79.63)	262 (82.39)	0.626	40 (80)	166 (83.84)	0.518
Absent	11 (20.37)	56 (17.61)		10 (20)	32 (16.16)	
Present						
Associated DCIS	33 (61.11)	241 (75.79)	0.024	36 (72)	144 (72.73)	0.918
Absent	21 (38.89)	77 (24.21)		14 (28)	54 (27.27)	
Present						
MF/MC disease	54 (100)	307 (96.54)	0.341	49 (98)	191 (96.46)	0.919
No	0 (0)	11 (3.46)		1 (2)	7 (3.54)	
Yes						
Histology type	51 (94.44)	295 (92.77)	0.874[e]	48 (96)	179 (90.40)	0.324[e]
IDC	1 (1.85)	11 (3.46)		1 (2)	8 (4.04)	
ILC	2 (3.70)	12 (3.77)		1 (2)	11 (5.56)	
Others[c]						
Type of surgery	53 (98.15)	269 (84.59)	0.007	50 (100)	172 (86.87)	0.007
Mastectomy	1 (1.85)	49 (15.41)		0 (0)	26 (13.13)	
BCS						

(Continued)

TABLE 2 | Continued

Characteristics	Training cohort (n = 372)			Validation cohort (n = 248)		
	High-risk (n = 54)	Low-risk (n = 318)	*P*-value	High-risk (n = 50)	Low-risk (n = 198)	*P*-value
Adjuvant endocrine therapy	20 (37.04)	93 (29.25)	0.250	18 (36)	67 (33.84)	0.774
No	34 (62.96)	225 (70.75)		32 (64)	131 (66.16)	
Yes						
Adjuvant chemotherapy	11 (20.37)	64 (20.13)	0.967	8 (16)	45 (22.73)	0.300
No	43 (79.63)	254 (79.87)		42 (84)	153 (77.27)	
Yes						
Adjuvant radiation	34 (62.96)	205 (64.47)	0.831	32 (64)	124 (62.63)	0.857
No	20 (37.04)	113 (35.53)		18 (36)	74 (37.37)	
Yes						
Adjuvant targeted therapy	44 (81.48)	271 (85.22)	0.481	42 (84)	166 (83.84)	0.978
No	10 (18.52)	47 (14.78)		8 (16)	32 (16.16)	
Yes						

Unless stated otherwise, data are numbers of patients, with percentages in parentheses.

[a]*Data represent mean ± standard deviations.*

[b]*History of risk factors for breast cancer include six patients with family history of breast cancer, 14 patients with benign breast disease history, one patient with breast lesion biopsy history.*

[c]*Other cancers include 13 mucinous carcinomas, five papillary carcinomas, three medullary carcinomas, two metaplastic carcinomas, one tubular carcinoma, one cribriform carcinoma, one apocrine carcinoma.*

[d]*P value is calculated after combining T3 and T4 as one group owing to the expected frequencies being <1.*

[e]*P value is calculated after combining ILC and Others as one group because more than 20% of the expected frequencies are less than 5.*

Rad-score, radiomics score; DCIS, ductal carcinoma in situ; MF, multifocal; MC, multicentric; IDC, invasive ductal carcinoma; ILC, invasive lobular carcinoma; BCS, breast conservation surgery.

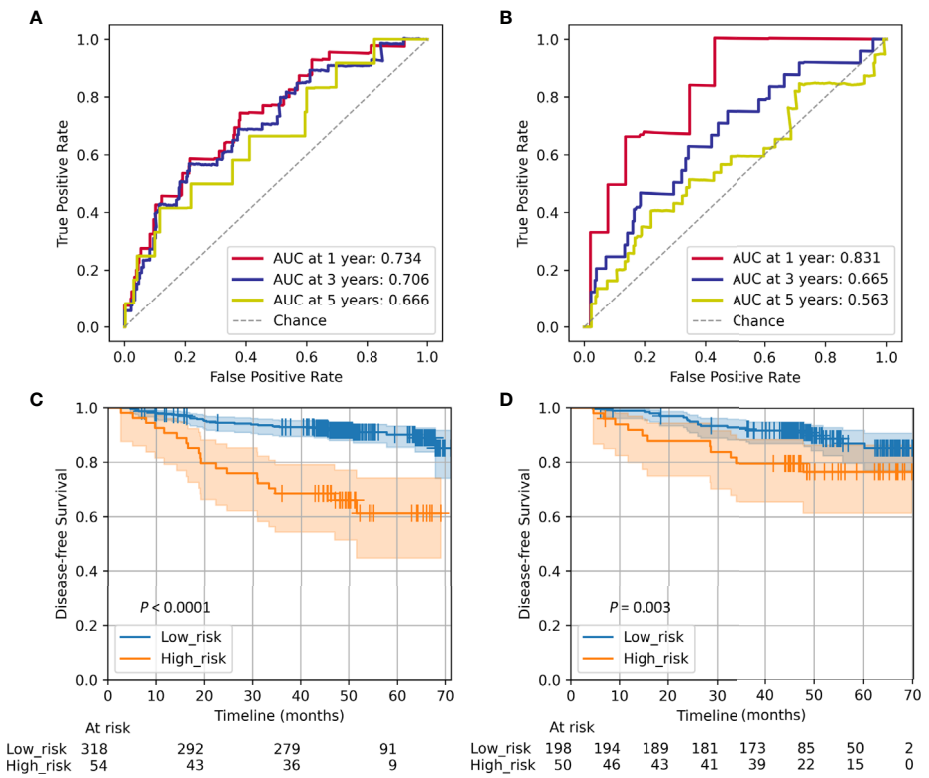

FIGURE 1 | Radiomics score measured by time-dependent ROC curves and Kaplan–Meier survival curves in the training and validation cohorts. We used AUCs at 1, 3, and 5 years to assess prognostic accuracy in the training **(A)** and validation **(B)** cohorts. A significant association of the Rad-score with DFS was shown in the training **(C)** and validation **(D)** cohorts. We calculated *P* values using the log-rank test. Data are the AUC or *P*-value. ROC, receiver operator characteristics; AUC, area under the curve; DFS, disease-free survival.

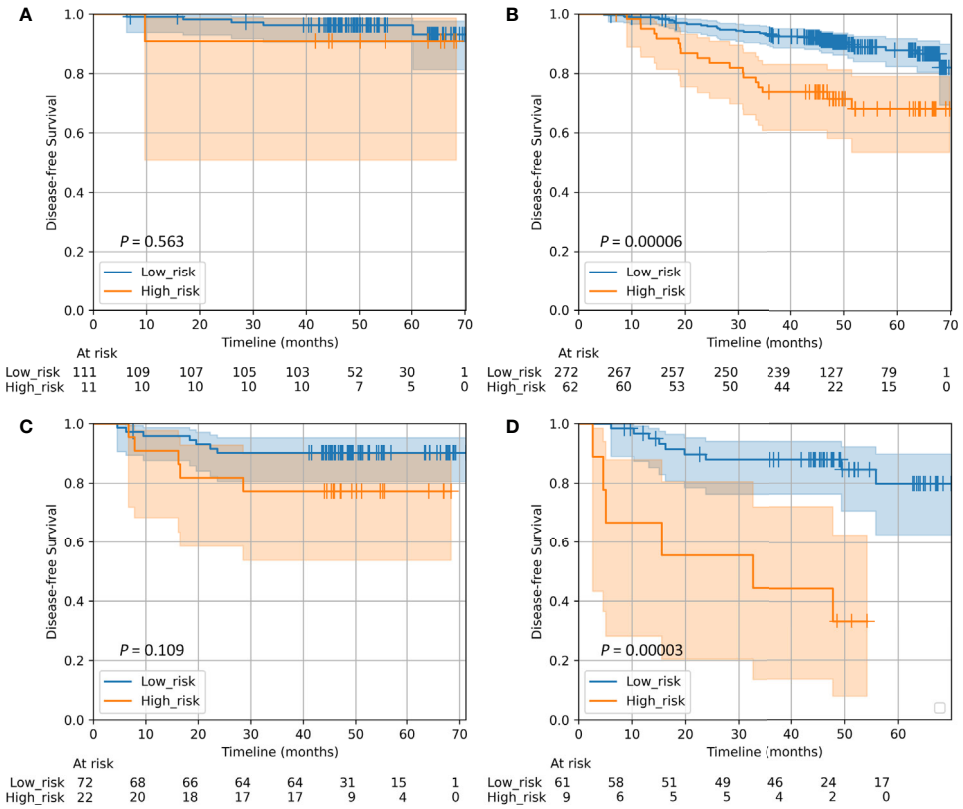

FIGURE 2 | Kaplan–Meier survival curves of DFS according to the Rad-score classifier in subgroups within molecular subtypes of patients with invasive breast cancer in the whole cohort. **(A)** Luminal A (n = 122). **(B)** Luminal B (n = 334). **(C)** HER2-enriched (n = 94). **(D)** Triple-negative (n = 70). We calculated *P* values using the log-rank test. DFS, disease-free survival; Rad-score, radiomics score.

Both in the univariate (**Table S3**) and multivariable analyses (**Table 3**), the Rad-score was an independent predictor for DFS.

The Additional Value of Radiomics Signature for DFS Prediction

The estimation of the radiomics nomogram achieved a better agreement with actual observation than that of the clinicopathological nomogram (**Figure 3**). The radiomics nomogram yielded the highest C-index (0.801 and 0.796 in the training and validation cohorts, respectively), the highest log likelihood (−241.70), and the lowest BIC (502.75) (**Table 4**). Including the radiomics signature to the clinicopathological nomogram resulted improvement of classification accuracy for survival outcomes, with a total NRI of 0.147 in the validation cohort for 5-year DFS estimation (**Table S4**). Finally, the results of DCA demonstrated that the radiomics nomogram was superior than the clinicopathological nomogram in terms of clinical usefulness both in the training and validation cohorts (**Figure 4**).

TABLE 3 | Multivariate analysis of DFS in the training cohort.

Variable	Hazard ratio (95% CI)	*P*-value
Rad-score	3.95 (1.87–8.37)	0.0003
Lymphovascular invasion		
Absent	reference	/
Present	2.19 (1.14–4.21)	0.018
Molecular subtype		
Luminal A	reference	/
Luminal B	2.04 (0.61–6.81)	0.247
HER2-enriched	3.12 (0.80–12.18)	0.031
Triple-negative	3.15 (0.75–12.43)	0.038
N stage		
0	reference	/
1	2.86 (1.21–6.73)	0.016
2	3.81 (1.46–9.97)	0.006
3	3.93 (1.15–12.31)	0.007
T stage		
1	Reference	/
2	1.46 (0.68–3.11)	0.332
3	2.90 (0.89–9.43)	0.076
4	0.80 (0.10–6.79)	0.842

Rad-score, radiomics score; CI, confidence interval.

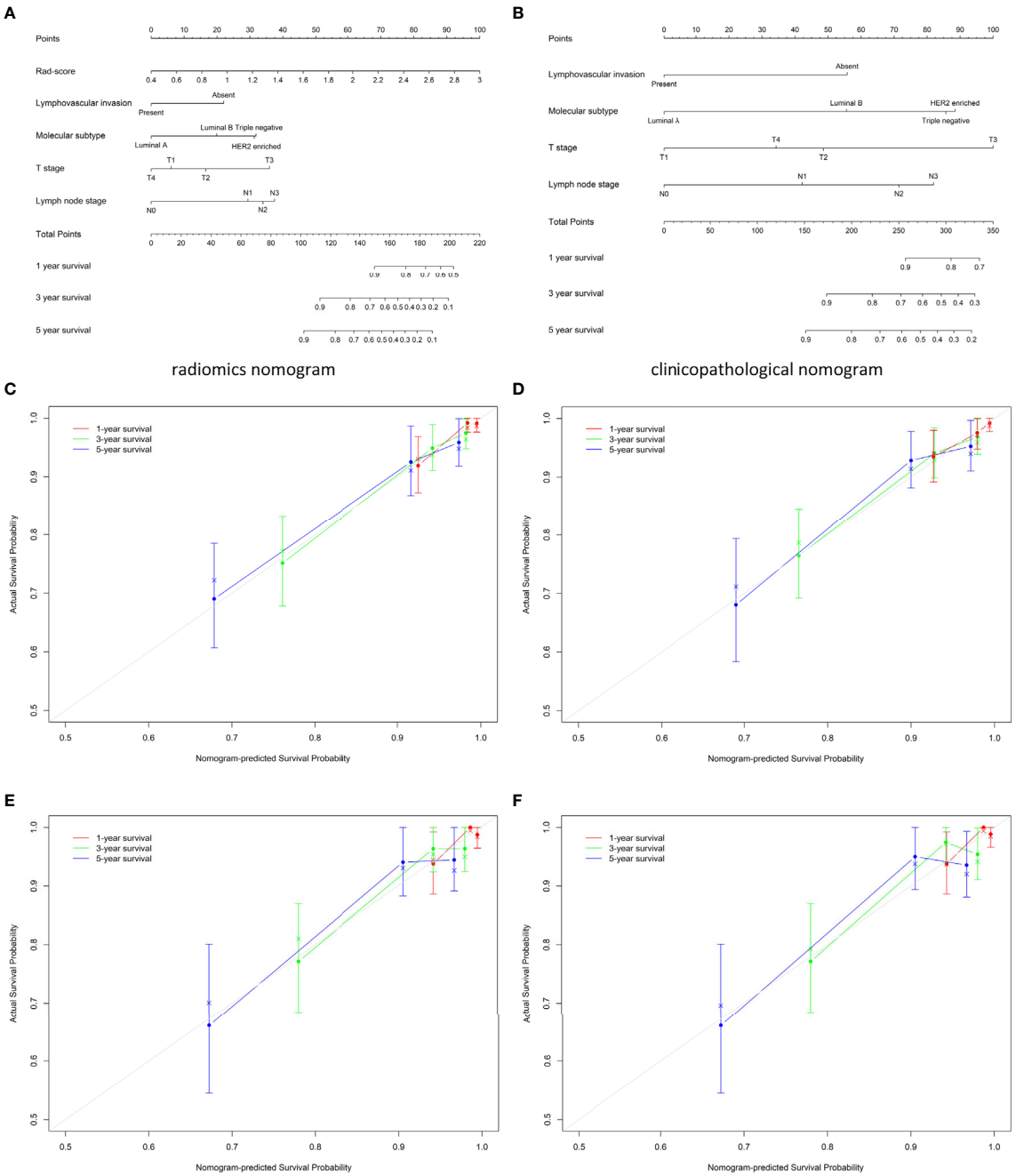

FIGURE 3 | The developed radiomics nomogram **(A)** and clinicopathological nomogram **(B)** for DFS prediction in patients with invasive breast cancer, along with the calibration curves of these nomograms. The patient's Rad-score is located on the Rad-score axis. To determine the number of points toward the probability of DFS the patient receives for her Rad-score, a line was drawn straight upward to the point axis, and this process was repeated for each variable. The points achieved for each of the risk factors was then summed. The final sum is located on the total point axis. To find the patient's probability of DFS, a line was drawn straight down. Calibration curves of the radiomics nomogram in the training **(C)** and validation **(E)** cohorts, and those of the clinicopathological nomogram in the training **(D)** and validation **(F)** cohorts show the calibration of each model in terms of the agreement between the estimated and observed at 1-, 3-, and 5-year outcomes. Nomogram-estimated probability is plotted on the x-axis, and the actual survival probability is plotted on the y-axis. The diagonal gray line represents a perfect estimation by an ideal model, in which the estimated outcome perfectly corresponds to the actual outcome. The colored line represents the nomogram's performance, a closer alignment of which with the diagonal dotted line represents a better estimation. DFS, disease-free survival; Rad-score, radiomics score.

TABLE 4 | Performance of models.

Model	C-index (95%CI)		BIC	Log likelihood	*P*-value
	Training cohort	Validation cohort			
Radiomics signature	0.714 (0.63–0.80)	0.632 (0.52–0.74)	521.80	–258.97	<0.0001[a]
Clinicopathological nomogram	0.771 (0.69–0.85)	0.761 (0.66–0.86)	511.42	–247.97	<0.001[b]
Radiomics nomogram	0.801 (0.72–0.88)	0.796 (0.70–0.89)	502.75	–241.70	/

[a]*The likelihood ratio test was performed between the radiomics signature and the radiomics nomogram.*
[b]*The likelihood ratio test was performed between the clinicopathological nomogram and the radiomics nomogram.*

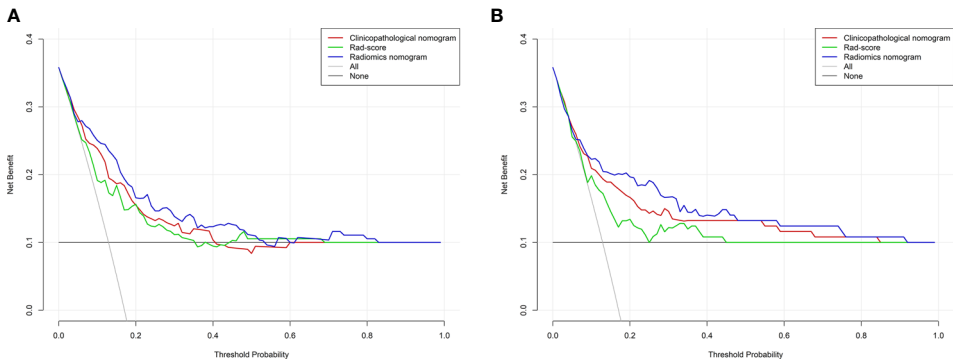

FIGURE 4 | Decision curve analysis for each model in the training **(A)** and validation **(B)** cohorts. The y-axis measures the net benefit. The net benefit was calculated by summing the benefits (true positive results) and subtracting the harms (false positive results), weighing the latter by a factor related to the relative harm of an undetected cancer compared with the harm of unnecessary treatment. The radiomics model had the highest net benefit and simple strategies such as follow-up of all patients (gray line) or no patients (horizontal black line) across the full range of threshold probabilities at which a patient would choose to undergo imaging follow-up.

Subgroup Analyses Based on Ultrasound Machines

As shown in **Figure S11**, higher Rad-scores were significantly associated with worse DFS in the GE subgroup ($P = 0.0001$), but not in the Mindray subgroup ($P = 0.055$). Patients with higher Rad-scores experienced worse DFS than patients with lower Rad-scores in both the subgroups. Based on the cutoff (1.816) of the Rad-score, these patient characteristics based on risk group are shown in **Table S5**.

DISCUSSION

To our knowledge, this study has developed the first US radiomics features for DFS prediction of invasive breast cancer. We showed that the US radiomics signature was an independent factor in predicting DFS and confirmed its additional value added to the clinicopathological predictors.

The present radiomics signature comprised 14 features, including two 2D shape-based features, seven texture features, and five wavelet features. On the one hand, shape-based features reflect the shape and morphology of the tumor. Being consistent with a previous study which selected surface to volume ratio (SVR) to estimate breast cancer DFS (17), we selected PerimeterSurfaceRatio feature (the 2D form of SVR) as one of the 14 features. On the other hand, texture analysis is a suitable way to assess tumor heterogeneity (26), and different texture features are defined differently to depict specific aspects of tumor textural heterogeneity and thus may provide complementary information of tumor characteristics. Most texture and wavelet features selected in the present study could describe characteristics of breast cancer in previous study (12). Thus, the multiple-feature-based radiomics signature constructed in our study could likely be an important prognostic factor with the information of tumor heterogeneity.

In the following analyses, the radiomics signature showed moderate performance on DFS prediction and successfully stratified patients into different groups according to the results of risk stratification, though there was only one selected feature could stratify the risk of DFS. These findings were similar to a previous study of lung cancer which demonstrated that no individual feature could classify patients at different risk of recurrence, except for radiomics signature (27). Therefore, the radiomics signature, taking the interactions between different features into account, could better reflect the heterogeneity of tumor and is thus related to the outcome of patient, improving the accuracy of DFS assessment.

In the subsequently univariate, multivariate, and stratified analyses, the present US radiomics signature was an independent predictor, indicating the strong association between the

radiomics signature and DFS. Patients at high-risk group experienced worse DFS than those at low-risk group, implying that patients at high risk of DFS might need more intensive treatment and follow-up to improve DFS, whereas treatment for low-risk patients could be attenuated appropriately. Consequently, our results would provide valuable information for clinicians to develop personalized treatment accurately based on the specific clinicopathological factors and radiomics signature for invasive breast cancer.

The Kaplan-Meier analyses performed by molecular subtype showed that only differences of DFS in luminal B and triple-negative subgroups were statistically significant. This suggested that the ability of radiomics signature to assess DFS for invasive breast cancer vary by molecular subtype, which was similar to an earlier MRI-based study (28). This also highlighted the fact that breast cancer is a heterogeneous tumor wherein every subtype has its unique characteristics and prognosis. Perhaps a specific radiomics signature for each molecular subtype would predict DFS better in invasive breast cancer and hence, further studies are needed to confirm this speculation.

Furthermore, we confirmed the additional value of radiomics signature to the clinicopathological predictors for DFS prediction. The single predictor is not enough to assess the probability of prognosis, whereas nomogram has the ability to integrate multiple factors. We constructed a radiomics nomogram in a step-wise manner based on BIC, achieving better performance compared to the clinicopathological nomogram, with a better calibration, positive NRI and higher C-index. Finally, the radiomics nomogram performed better than the clinicopathological nomogram in term of clinical usefulness, which confirmed the additional value of the radiomics signature for personalized DFS prediction in patients with invasive breast cancer simultaneously.

Finally, we analyzed whether different sonographic platforms affect the performance of radiomics signature and radiomics signature showed significant only in the GE subgroup. We think this may be related to small sample size of the Mindray subgroup (n = 121). Small sample size generally affects the performance of radiomics study (29). Taking small sample size into consideration, radiomics signature shows significant association with DFS in the Mindray subgroup when relax the significant *P* value to 0.1. Furthermore, the significant clinicopathological variables (tumor size, T stage, N stage, TNM stage and LVI) showed consistent in the GE and Mindray subgroups according to risk group based on radiomics signature. However, the probability of the dependency of radiomics signature on the type of US machine could not be entirely rule out and further studies with larger data are needed to reveal the truth of this problem.

Our study has some limitations. First, we could not control the operator dependency or scanning parameters in collecting US images, which is an inevitable issue. So, we used Z-score normalization to minimize the influence of contrast and brightness variation before feature extraction for each patient. Second, radiomics signature showed dependency on the type of US machine in present study. Third, this study had a relatively short follow-up period (median follow-up, 48.99 months) and no independent validation. Thus, further studies with a longer follow-up, independent data and larger sample size are needed to resolve these issues.

In summary, the US radiomics signature is a potential imaging predictor for risk stratification of DFS, the radiomics nomogram holds promise to serve as a noninvasive tool to assist clinicians in accurately developing personalized treatment for patients with invasive breast cancer.

DATA AVAILABILITY STATEMENT

The raw data supporting the conclusions of this article will be made available by the authors, without undue reservation.

ETHICS STATEMENT

This study has obtained the ethical approval from the institutional review board of Sun Yat-Sen University Cancer Center.

AUTHOR CONTRIBUTIONS

LozL and LiL: guarantor of the article. LozL, LiL, LX, HC, and XT: conception and design. LX, HC, XT, BC, XJ, and LizL: collection and assembly of data. LX, HC, XT, and YF: data analysis and interpretation. All authors contributed to the article and approved the submitted version.

FUNDING

We acknowledge support from the Science and Technology Planning Project of Guangdong Province (2017B020226004), the Science and Technology Program of Guangzhou (201807010057, 201907010043), and the Health and Medical Collaborative Innovation Project of Guangzhou (201803010021), and the Youth Fund Project of Guangdong Basic and Applied Basic Research Fund Regional Joint Fund (2020A1515110939).

SUPPLEMENTARY MATERIAL

The Supplementary Material for this article can be found online at: https://www.frontiersin.org/articles/10.3389/fonc.2021.621993/full#supplementary-material.

REFERENCES

1. Ferlay J, Colombet M, Soerjomataram I, Mathers C, Parkin DM, Piñeros M, et al. Estimating the Global Cancer Incidence and Mortality in 2018: GLOBOCAN Sources and Methods. *Int J Cancer* (2019) 144:1941–53. doi: 10.1002/ijc.31937
2. Wang X, Wang N, Zhong L, Wang S, Zheng Y, Yang B, et al. Prognostic Value of Depression and Anxiety on Breast Cancer Recurrence and Mortality: A Systematic Review and Meta-Analysis of 282,203 Patients. *Mol Psychiatry* (2020) 25:3186–97. doi: 10.1038/s41380-020-00865-6
3. Goss PE, Ingle JN, Pritchard KI, Robert NJ, Muss H, Gralow J, et al. Extending Aromatase-Inhibitor Adjuvant Therapy to 10 Years. *N Engl J Med* (2016) 375:209–19. doi: 10.1056/NEJMoa1604700
4. Phung MT, Tin Tin S, Elwood JM. Prognostic Models for Breast Cancer: A Systematic Review. *BMC Cancer* (2019) 19:230. doi: 10.1186/s12885-019-5442-6
5. Syed YY. Oncotype DX Breast Recurrence Score®: A Review of its Use in Early-Stage Breast Cancer. *Mol Diagn Ther* (2020) 24:621–32. doi: 10.1007/s40291-020-00482-7
6. Reig B, Heacock L, Geras KJ, Moy L. Machine Learning in Breast MRI. *J Magn Reson Imaging* (2020) 52:998–1018. doi: 10.1002/jmri.26852
7. Li H, Zhu Y, Burnside ES, Drukker K, Hoadley KA, Fan C, et al. Mr Imaging Radiomics Signatures for Predicting the Risk of Breast Cancer Recurrence as Given by Research Versions of MammaPrint, Oncotype DX, and PAM50 Gene Assays. *Radiology* (2016) 281:382–91. doi: 10.1148/radiol.2016152110
8. Huang SY, Franc BL, Harnish RJ, Liu G, Mitra D, Copeland TP, et al. Exploration of PET and MRI Radiomic Features for Decoding Breast Cancer Phenotypes and Prognosis. *NPJ Breast Cancer* (2018) 16:4:24. doi: 10.1038/s41523-018-0078-2
9. Chitalia RD, Rowland J, McDonald ES, Pantalone L, Cohen EA, Gastounioti A, et al. Imaging Phenotypes of Breast Cancer Heterogeneity in Preoperative Breast Dynamic Contrast Enhanced Magnetic Resonance Imaging (Dce-Mri) Scans Predict 10-Year Recurrence. *Clin Cancer Res* (2020) 26:862–9. doi: 10.1158/1078-0432.CCR-18-4067
10. Youk JH, Kwak JY, Lee E, Son EJ, Kim JA. Grayscale Ultrasound Radiomic Features and Shear-Wave Elastography Radiomic Features in Benign and Malignant Breast Masses. *Ultraschall Med* (2020) 41:390–6. doi: 10.1055/a-0917-6825
11. Yu FH, Wang JX, Ye XH, Deng J, Hang J, Yang B. Ultrasound-Based Radiomics Nomogram: A Potential Biomarker to Predict Axillary Lymph Node Metastasis in Early-Stage Invasive Breast Cancer. *Eur J Radiol* (2019) 119:108658. doi: 10.1016/j.ejrad.2019.108658
12. Guo Y, Hu Y, Qiao M, Wang Y, Yu J, Li J, et al. Radiomics Analysis on Ultrasound for Prediction of Biologic Behavior in Breast Invasive Ductal Carcinoma. *Clin Breast Cancer* (2018) 18:e335–44. doi: 10.1016/j.clbc.2017.08.002
13. Hammond ME, Hayes DF, Dowcohortt M, Allred DC, Hagerty KL, Badve S, et al. American Society of Clinical Oncology/College of American Pathologists Guideline Recommendations for Immunohistochemical Testing of Estrogen and Progesterone Receptors in Breast Cancer (Unabridged Version). *Arch Pathol Lab Med* (2010) 134:e48–72. doi: 10.1043/1543-2165-134.7.e48
14. Wolff AC, Hammond ME, Hicks DG, Dowcohortt M, McShane LM, Allison KH, et al. Recommendations for Human Epidermal Growth Factor Receptor 2 Testing in Breast Cancer: American Society of Clinical Oncology/College of American Pathologists Clinical Practice Guideline Update. *Arch Pathol Lab Med* (2014) 138:241–56. doi: 10.5858/arpa.2013-0953-SA
15. Goldhirsch A, Wood WC, Coates AS, Gelber RD, Thürlimann B, Senn HJ. Panel Members. Strategies for Subtypes–Dealing With the Diversity of Breast Cancer: Highlights of the St. Gallen International Expert Consensus on the Primary Therapy of Early Breast Cancer 2011. *Ann Oncol* (2011) 22:1736–47. doi: 10.1093/annonc/mdr304
16. Edge SB, Compton CC. The American Joint Committee on Cancer: The 7th Edition of the AJCC Cancer Staging Manual and the Future of TNM. *Ann Surg Oncol* (2010) 17:1471–4. doi: 10.1245/s10434-010-0985-4
17. Park H, Lim Y, Ko ES, Cho HH, Lee JE, Han BK, et al. Radiomics Signature on Magnetic Resonance Imaging: Association With Disease-Free Survival in Patients With Invasive Breast Cancer. *Clin Cancer Res* (2018) 24:4705–14. doi: 10.1158/1078-0432.CCR-17-3783
18. Lynch SP, Lei X, Hsu L, Meric-Bernstam F, Buchholz TA, Zhang H, et al. Breast Cancer Multifocality and Multicentricity and Locoregional Recurrence. *Oncologist* (2013) 18:1167–73. doi: 10.1634/theoncologist.2013-0167
19. van Griethuysen JJM, Fedorov A, Parmar C, Hosny A, Aucoin N, Narayan V, et al. Computational Radiomics System to Decode the Radiographic Phenotype. *Cancer Res* (2017) 77:e104–7. doi: 10.1158/0008-5472.CAN-17-0339
20. Tibshirani R. The Lasso Method for Variable Selection in the Cox Model. *Stat Med* (1997) 16:385–95. doi: 10.1002/(sici)1097-0258(19970228)16:4<385::aid-sim380>3.0.co;2-3
21. Gui J, Li H. Penalized Cox Regression Analysis in the High-Dimensional and Low-Sample Size Settings, With Applications to Microarray Gene Expression Data. *Bioinformatics* (2005) 21:3001–8. doi: 10.1093/bioinformatics/bti422
22. Camp RL, Dolled-Filhart M, Rimm DL. X-Tile: A New Bio-Informatics Tool for Biomarker Assessment and Outcome-Based Cut-Point Optimization. *Clin Cancer Res* (2004) 10:7252–9. doi: 10.1158/1078-0432.CCR-04-0713
23. Gonen M, Heller G. Concordance Probability and Discriminatory Power in Proportional Hazards Regression. *Biometrika* (2005) 92:965–70. doi: 10.1093/biomet/92.4.965
24. Pencina MJ, D'Agostino RB, Steyerberg EW. Extensions of Net Reclassification Improvement Calculations to Measure Usefulness of New Biomarkers. *Stat Med* (2011) 30:11–21. doi: 10.1002/sim.4085
25. Vickers AJ, Elkin EB. Decision Curve Analysis: A Novel Method for Evaluating Prediction Models. *Med Decis Making* (2006) 26:565–74. doi: 10.1177/0272989X06295361
26. Davnall F, Yip CS, Ljungqvist G, Selmi M, Ng F, Sanghera B, et al. Assessment of Tumor Heterogeneity: An Emerging Imaging Tool for Clinical Practice? *Insights Imaging* (2012) 3:573–89. doi: 10.1007/s13244-012-0196-6
27. Huang Y, Liu Z, He L, Chen X, Pan D, Ma Z, et al. Radiomics Signature: A Potential Biomarker for the Prediction of Disease-Free Survival in Early-Stage (I or II) non-Small Cell Lung Cancer. *Radiology* (2016) 281:947–57. doi: 10.1148/radiol.2016152234
28. Drukker K, Li H, Antropova N, Edwards A, Papaioannou J, Giger ML. Most-Enhancing Tumor Volume by MRI Radiomics Predicts Recurrence-Free Survival "Early on" in Neoadjuvant Treatment of Breast Cancer. *Cancer Imaging* (2018) 18:12. doi: 10.1186/s40644-018-0145-9
29. Park JE, Park SY, Kim HJ, Kim HS. Reproducibility and Generalizability in Radiomics Modeling: Possible Strategies in Radiologic and Statistical Perspectives. *Korean J Radiol* (2019) 20:1124–37. doi: 10.3348/kjr.2018.0070

Conflict of Interest: The authors declare that the research was conducted in the absence of any commercial or financial relationships that could be construed as a potential conflict of interest.